Design and Analysis of Planar Dual Mode Antenna Array

MSEE Project Report

By

Vikram Arora

	Signature	Date
Project Advisor:	_____	_____
	Professor Ray Kwok	
Project Co-Advisor:	_____	_____
	Professor Masoud Mostafavi	
Graduate Coordinator:	_____	_____
	Professor Peter Reischl	

Department of Electrical Engineering
San Jose State University
San Jose, CA 95192-0084

_____

Vikram Arora
004023644
1901 Halford Ave, Apt 149, Santa Clara,
CA 95051
408-615-1473
vikram_ar@yahoo.com

Abstract

Planar microstrip patch antennas are the preferred choice of antennas for printed circuit boards due to their low profile, mechanical ruggedness, easy mounting and low cost. There are two categories of simulation software available for analysis of patch antennas, Full Wave Models based and Analytical Models based. Full Wave Models based software take the rigorous approach, and produce good accuracy, but cost thousands of dollars, have significant learning curves and parametric analysis can take hours. Analytical Models based approach makes one or more significant approximations to simplify the problem. The results have lesser accuracy especially with thick substrates, but parametric variations can be solved very quickly, which helps with gaining insight into underlying physics. Special purpose user interface for specific application can be developed leading to very small learning curve for user, and development cost is significantly lower. Not many commercial analytical models based softwares with friendly user interface are available, and command line interface has only limited usefulness. In this project Matlab Graphical User Interface based patch antenna simulation software with array simulation capability has been developed. The software has the capability to predict return loss, circular polarization, radiation pattern based upon cavity model and allow simulation of antenna array. A dual band antenna has been fabricated and the results have been compared with simulation results. The measurement results show good agreement with simulation results within the tolerance of fabrication and experiment method.

Acknowledgements

I owe my thanks to my advisors:

Prof. Ray Kwok: Thanks for your constant support, encouragement, guidance, sharing your wisdom, and always being there to help out.

Prof. Masoud Mostafavi: Thanks for your enthusiasm for project, feedback and advice.

I would like to thank Irma Alarcon for her help and support in E347 lab.

I owe a special gratitude to my wife, Ritu, and my newborn, Megha, thanks for being my motivation. Finally a special thanks to my family in India – my parents and my sister, Meena, thanks for your constant encouragement.

Table of Contents

List of Figures

List of Tables

– Rotation around Y axis

– Antenna rotate 90_0 around X axis, Rotation around Y axis

– Axial Ratio, Rotation around Z axis

1. Introduction

The tremendous growth in the wireless communication in the commercial systems has produced the need for antennas, which are low in cost and easier to fabricate and integrate with other microwave components. Planar microstrip patch antennas are the preferred choice of antennas for printed circuit boards due to their low profile, mechanical ruggedness, easy mounting, low cost and ease of integration with other microwave devices in microstrip technology. Both linear and circular polarizations are possible. Numerous advancements have occurred in the microstrip antenna technology in past few decades that has enabled their widespread use in personal communication systems, mobile satellite communications and wireless local area networks (WLANs) [14].

Microstrip antennas have some limitations also. They are inherently narrow band, have low gain, and polarization purity is typically low. [3]. Some of these limitations can be overcome with specific techniques e.g bandwidth can be increased by increasing the substrate height.

1.1 Characteristics of Microstrip Patch Antennas

Microstrip antennas consist of a patch of metallization over ground plane separated by a dielectric substrate. They are commonly referred to as patch antennas also. The thickness of substrate, h is usually very small compared to λ_0, the free space wavelength, the typical range being, $0.003\lambda_0 \leq h \leq 0.05\lambda_0$ [5]. Patch antennas are normally broadside antennas, although it is possible to design end fire radiation also. The length of patch is typically order of $\lambda_0/2$ i.e $L \approx \lambda_0/2$. Numerous shapes of patch geometry has been studied and used

1
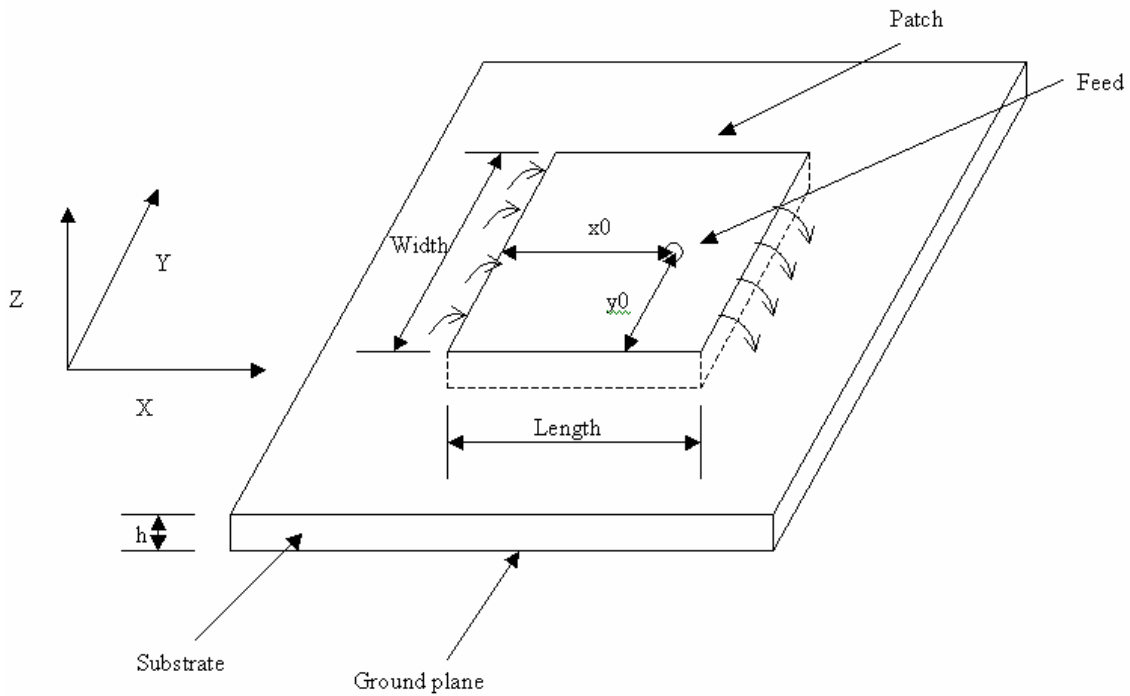
Figure 1.1: Microstrip Patch Antenna

in patch antennas over past few decades e.g rectangular, circular, elliptical and triangular

[3]. Rectangular and circular seems to be the most often used geometries for patch. The

rectangular geometry has been investigated in this project.

A large number of substrates can be used for microstrip patch antennas. The

dielectric constant is typically in the range, $2.2 \leq \varepsilon_r \leq 12$ [5]. The substrates with low

dielectric constant produce better radiation efficiency due to loosely bound fields, but end

up larger size of patch. On the other hand, substrates with higher dielectric constants lead

of small patch sizes, but are less efficient radiators due to tightly bound fields. A compromise needs to be reached owing to other considerations e.g integration with other microwave components.

Both linear and circular polarizations can be achieved with microstrip patch antennas. Array of patch antennas can be used in order to increase the directivity or to have scanning capabilities.

1.2 Methods of Feeding

The two most common methods of feeding microstrip patch antennas are microstrip line and coaxial probe. A number of other methods have been developed also e.g proximity-coupled microstrip feed, aperture coupled microstrip feed and coplanar waveguide feed [3]. The major requirement from the feed is the efficient transfer of power from feed to antenna. Typically the impedance matching criteria along with other considerations like feeding of array arrangements dictate the selection and design of feed. The coaxial feed has been used in this project. N type coaxial connector is typically used, in which the connector is attached to the back side (ground plane) of antenna and coaxial center conductor is passed through the substrate and soldered to the patch element.

1.3 Principle of Operation

The basic mechanism of radiation of patch antenna is the fringing of fields beyond the edges of patch element, as shown in Figure 1.1. The feeding of patch antenna produces the current density and electric and magnetic fields in the region between patch element and ground plane, the fields fringe beyond the physical dimensions of patch, and these

fringe fields produce the radiation. The amount of fringing of fields depends upon the dimensions of patch, and the height and dielectric constant of substrate. The increase in height of substrate causes increase in fringe fields. The higher dielectric constant of the substrate binds the fields more tightly inside the substrate region between patch and ground plane and reduces the fringe fields. More the amount of fringing, better would be the radiation efficiency of patch antenna.

2. Modeling of Microstrip Patch Antenna

A large number of methods have been developed to model the microstrip patch antenna. A good model of antenna should be able to predict the desired electrical characteristics of antenna with accurate enough results for the given purpose, and should be able to do that in computationally efficient way. Other desirable characteristics of the model are reasonably fast solutions for parametric variations of design parameters and user-friendly interface. Most of the models developed so far for patch antennas can be divided into two categories a) Full Wave Models b) Analytical Models [14].

2.1 Full Wave Models

The full wave models for microstrip patch antennas take the rigorous approach and accurately models the dielectric substrate. They produce very accurate solutions, however computational cost is typically quite high. The solutions for parametric variations can take hours of simulation time. There are three types of approaches used for full wave models a) Method of Moments (MoM) b) Finite Difference Time Domain (FDTD) c) Finite Element Method (FEM). The MoM approach assumes the substrate to be infinite and model it with exact Greens functions. The patch and ground plane conductors are modeled with basis functions. FDTD and FEM are brute force kind of methods, the entire structure is subdivided and modeled with basis functions. These two methods have the capability to handle any shape of the structure, however they are computationally very expensive. A large number of commercial software based upon full wave models have become available in market, a partial list can be found in chapter 1 of [14].

2.2 Analytical Models

The analytical models for microstrip antenna make one or more significant approximations to greatly simplify the problem. This typically allows the derivation of closed form equations with the result that solutions can be computed with much lesser computation expense as compared to full wave models. However this also implies that the computed solutions are less accurate. There are two main types of analytical models developed for patch antennas a) Transmission Line Model and b) Cavity Model. The few variants and generalizations of these approaches have also been developed [3].

The transmission line based approach models the region between patch and ground plane as a section of transmission line of length, L. The dimensions of patch and substrate parameters determine the characteristic impedance and propagation constant of transmission line.

The cavity model based approach models the region between patch and ground plane as cavity with electric walls on top and bottom, and magnetic walls along the periphery. The dimensions of patch and substrate parameters determine the modes of the cavity.

2.3 Comparison between Full Wave Models and Analytical Models

The full wave models based software for antenna analysis produce very accurate results, and are capable of predicting all characteristics of antenna e.g resonance frequency, return loss as function of frequency sweep, radiation pattern and cross polarizations. However they are computationally very expensive, and cost thousands of dollars. They are typically general purpose Electromagnetic Analysis software and there is a significant

learning curve to use the interface for given antenna design. On the other hand, analytical model based software can solve parametric variations quickly, which helps in gaining the physical insight into the underlying physics of the problem. The results are less accurate, however accuracy might be sufficient for the given application. Specific user interface can be developed which would mean a very short or negligible learning curve. A few such software are available, but number of them are command line based, which has limited usefulness [8]. In this project, we propose to write a Matlab GUI based software for analytical modeling of patch antenna. The software is to have the following abilities

    a) Ability to simulate return loss v/s frequency sweep

    b) Ability to predict circular polarization (CP)

    c) Ability to simulate dual band antenna

    d) Ability to simulate radiation pattern

    e) Ability to simulate antenna array

2.4 Comparison between Transmission Line Model and Cavity Model

The transmission line model is simple but it produces acceptable results only when the feed point is near the radiating edges [2]. A fundamental drawback of this model is that it does not account for non-resonant modes while predicting the input impedance of the antenna.

      The cavity model on the other hand, is based upon the modal expansion technique and it incorporates the affect of non-resonant modes on the input impedance. The results computed using the cavity model has closer agreement with experimental results even when the feed point is away from the edges of the patch. It is also possible to predict

circular polarization using the cavity model. The mathematical formulation of cavity

model is little bit more complex that transmission line model, but it is possible to derive

the closed form expressions, with the result that computational efficiency is not sacrificed

much.

   In this project we propose to use the cavity model for the patch antenna in Matlab

GUI based software.

3. Cavity Model for Microstrip Patch Antenna

The cavity model for analyzing the patch antenna was proposed by Richards, Lo and others [6]. Further improvements have been proposed since then [7][9][10]. The region of substrate between patch and ground plane, termed as interior region, is modeled a cavity, bounded by electric walls on top and bottom and magnetic walls along the periphery. The substrate is assumed to be thin i.e $h \ll \lambda_0$. The fields in the interior region are assumed not to vary along z direction i.e $\partial/\partial z = 0$, see Figure 1.1 for coordinate system definition.

3.1 Electric Wall Boundary Condition

The patch and ground plane are assumed to be perfect conductors, and assumed to represent electric wall. The boundary conditions for electric wall are [6]

$$\hat{n} \bullet \vec{D} = \rho_s \tag{3.1a}$$
$$\hat{n} \bullet \vec{B} = 0 \tag{3.1b}$$
$$\hat{n} \times \vec{E} = 0 \tag{3.1c}$$
$$\hat{n} \times \vec{H} = \vec{J}_s \tag{3.1d}$$

The electric wall assumption implies that the tangential component of E field is zero, and it has only normal component i.e E_z in our case. Additionally normal component of magnetic field is zero, and it has only tangential components i.e H_x and H_y in our case.

3.2 Magnetic Wall boundary Condition

The interior region between patch and ground plane is assumed to be bounded by magnetic wall along the periphery. The boundary conditions for magnetic wall are [6]

$$\hat{n} \cdot \vec{D} = 0 \qquad (3.2a)$$
$$\hat{n} \cdot \vec{B} = 0 \qquad (3.2b)$$
$$\hat{n} \times \vec{E} = -\vec{M}_s \qquad (3.2c)$$
$$\hat{n} \times \vec{H} = 0 \qquad (3.2d)$$

The magnetic wall assumption implies E field normal to the periphery and H field tangential to the periphery are zero.

The above boundary condition assumptions lead to the assumption that only non-zero field components are E_z, H_x and H_y.

3.3 Input Impedance

The input impedance for a given feed location is computed by first computing the E field based upon the modes of cavity and then artificially introducing the radiation as a loss component along with dielectric and conductor loss [3].

With only E_z, H_x and H_y as non zero field components, the wave equation becomes

$$\frac{\partial^2 E_z}{\partial x^2} + \frac{\partial^2 E_z}{\partial y^2} + k^2 E_z = j\omega\mu_0 J \qquad (3.3)$$
$$k^2 = \omega^2 \mu_0 \varepsilon_0 \varepsilon_r$$

J is the feed current. The feed is assumed to be coaxial in this project.

The electric field is then expressed in terms of various modes of cavity

$$E_z(x, y) = \sum_m \sum_n A_{mn} \psi_{mn}(x, y) \qquad (3.4)$$

where A_{mn} are amplitude coefficients of orthonormalized eigenfunctions ψ_{mn}. The eigenfunction ψ_{mn} must satify the wave equation and following boundary conditions and normalization conditions

$$\frac{\partial \psi_{mn}}{\partial x} = 0 \; at \; x = 0 \; and \; x = L \quad (3.5a)$$

$$\frac{\partial \psi_{mn}}{\partial y} = 0 \; at \; y = 0 \; and \; y = W \quad (3.5b)$$

$$(\frac{\partial^2}{\partial x^2} + \frac{\partial^2}{\partial x^2} + k_{mn}^2) \psi_{mn} = 0 \qquad (3.5c)$$

$$\iint_{x \; y} \psi_{mn} \psi_{mn}^* \, dxdy = 1 \qquad (3.5d)$$

Solving equations 3a to 3d gives

$$\psi_{mn}(x, y) = \sqrt{\frac{\varepsilon_m \varepsilon_m}{LW}} \cos(k_m x) \cos(k_n y) \quad m, n = 0,1,2, p... \quad (3.6)$$

$$\varepsilon_p = 1, if \; p = 0$$

$$\varepsilon_p = 2, if \; p \neq 0$$

$$k_m = m\pi / L, \; k_n = n\pi / W, k_{mn}^2 = k_m^2 + k_n^2$$

The next step is to determine A_{mn}. Feed current determines them, so we need to model the feed. Substituting equation 3.6 into 3.4, multiplying both sides of 3.4 with ψ^*_{mn}, integrating over the area of patch, and making use of 3.5a to 3.5d, we obtain [3]

11

$$A_{mn} = \frac{j\omega\mu_0}{k^2 - k_{mn}^2} \iint_{feed} \psi_{mn}^* J_z \, dxdy \qquad (3.7)$$

The feed model used in this project is the uniform current density over rectangular cross section, D_xD_y with area of rectangular cross section equal to actual cross sectional area of probe [3].

$$J_z = I_0 / D_x Dy, \quad x_0 - D_x/2 \le x \le x_0 + D_x/2 \; and \; y_0 - D_y/2 \le y \le y_0 + D_y/2 \qquad (3.8)$$
$$J_z = 0, \; elsewhere$$

Using 3.8 in 3.7 gives

$$A_{mn} = \frac{1}{D_x D_y} \frac{j\omega\mu_0}{k^2 - k_{mn}^2} \iint_{feed} I_0 \psi_{mn}^* \, dxdy$$

$$= \frac{j\omega\mu_0}{k^2 - k_{mn}^2} \sqrt{\frac{\varepsilon_m \varepsilon_n}{LW}} \cos(k_m x_0) \cos(k_n y_0) G_{mn} \qquad (3.9)$$

$$\text{where,} \; G_{mn} = \sin c(n\pi D_x /(2L)) \sin c(n\pi D_y /(2W)) \qquad (3.10)$$

Inserting 3.6 and 3.9 in 3.4 gives

$$E_z(x, y) = j\omega\mu_0 I_0 \sum_{m=0}^{\infty} \sum_{n=0}^{\infty} \frac{\psi_{mn}(x, y)\psi_{mn}(x_0, y_0)}{k^2 - k_{mn}^2} G_{mn} \qquad (3.11)$$

Based upon the E field computed above input impedance can be computed as follows

$$Z_{in} = \frac{V_{in}}{I_0} \qquad (3.12)$$

$$V_{in} = -E_z(x_0, y_0)h \qquad (3.13)$$

$$Z_{in} = -j\omega\mu_0 h\sum_{m=0}^{\infty}\sum_{n=0}^{\infty}\frac{\psi_{mn}^2(x_0, y_0)}{k^2 - k_{mn}^2}G_{mn} \qquad (3.14)$$

where $k^2 = \omega^2\mu_0\varepsilon_0\varepsilon_r$

3.3.1 Incorporating Losses

If we do not include the losses in equation 3.14, input impedance would be purely reactive as all the quantities under the summation sign are real. The dielectric losses as well as radiation losses need to be incorporated in order to correctly predict the input impedance. The typical method to incorporate losses is to replace $\varepsilon_0\varepsilon_r$ by $\varepsilon_0\varepsilon_r(1 - j \tan \delta)$, where $\tan \delta$ is the loss tangent of the substrate. The radiation loss can accounted for by artificially increasing the loss tangent term [2].

$$\delta_{eff} = \tan\delta + \frac{\Delta}{h} + \frac{P_r}{\omega W_T} \qquad (3.15)$$

δ : substrate loss tangent, Δ : skin depth, $\tan\delta \approx \dfrac{\varepsilon''}{\varepsilon'}$

P_r : Radiated power, W_T : Time averaged total energy stored under patch

Accounting for losses in 3.4 yields

$$Z_{in} = -j\omega\mu_0 h\sum_{m=0}^{\infty}\sum_{n=0}^{\infty}\frac{\psi_{mn}^2(x_0,y_0)}{k_0^2\varepsilon_r(1-j\delta_{eff})-k_{mn}^2}G_{mn} \qquad (3.16)$$

The radiated power, P_r can be computed by integrating the far fields as in [8], however [8] also describes approximating the sin and cos terms in far field expressions with polynomial, doing the analytical integration and coming up with following for P_r

$$P_r = \frac{V_0^2 A\pi^4}{23040}\left[(1-B)(1-\frac{A}{15}+\frac{A^2}{420})+\frac{B^2}{5}(2-\frac{A}{7}+\frac{A^2}{189})\right] \qquad 3.17$$

where $A = \left(\frac{\pi L}{\lambda_0}\right)^2$

and $B = \left(\frac{2W}{\lambda_0}\right)^2$

The stored electric energy, at resonance for dominant mode, is given by [8]

$$W_T = \frac{\varepsilon_0\varepsilon_r LWV_0^2}{8h} \qquad (3.18)$$

The equations 3.17 and 3.18 can be used in 3.15 to compute δ_{eff}, which then can be used to compute input impedance from 3.16.

3.3.2 Accounting for fringing of fields

It was mentioned in chapter 1 that fields in the region between the patch and ground plane extend beyond the physical dimensions of the patch. This phenomenon is called fringing of fields and is actually responsible for the radiation from patch antenna. The fringing of fields makes the patch look electrically larger than its physical dimensions. The affect of fringing of fields has originally been accounted for in transmission line model [5] , but has been proposed to use in cavity model also [9].

Since a portion of fields exist in the substrate and a portion in the air, the concept of effective dielectric constant, ε_{reff} is introduced [5]. The effective dielectric constant is given by

$$\varepsilon_{reff} = \frac{\varepsilon_r + 1}{2} + \frac{\varepsilon_r - 1}{2}\left[1 + 12\frac{h}{W}\right]^{-1/2} \qquad (3.19)$$

The effective dielectric constant is then used to find the extension of length, ΔL on each side and effective length, L_{eff} [5][9]

$$\frac{\Delta L}{h} = 0.412\frac{(\varepsilon_{reff} + 0.3)(\frac{W}{h} + 0.264)}{(\varepsilon_{reff} - 0.258)(\frac{W}{h} + 0.8)} \qquad (3.20)$$

$$L_{eff} = L + 2\Delta L \qquad (3.21)$$

The effective length, L_{eff} is used in place of L to compute input impedance.

15

3.4 Circular Polarization

One of the requirements mentioned for the proposed software is to be able to predict and design for circular polarization. Circular polarization is achieved in rectangular patch antennas by exciting two orthogonal modes, which are, equal in amplitude but differ by 90° in phase difference. There are two fundamentally different methds of achieving this. The first method involves exciting two orthogonal modes with a single feed and perturbing the dimensions or interior of patch in such a way that the magnitudes of two modes are essentially equal, but they have 90° phase difference. This is often referred to as singly-fed patch. The second method involves directly feeding two orthogonal modes with a device that provides equal amplitude and 90° phase difference [13]. The second method involves extra microwave circuitry and is hence expensive. We propose to use the first method in this project.

3.4.1 Circular Polarization with Singly Fed Patch

There are multiple ways of obtaining circular polarization with singly fed patch antenna also. One method is to remove a pair of corners and adjust the dimensions of cut outs to excite orthogonal modes with equal magnitude but 90° phase difference. In another method, the design starts with a square patch, then the dimensions of square patch are perturbed and patch is fed at a point on or close to the one of the diagonal, such that two degenerate modes TM_{01} and TM_{10} are excited with equal magnitude but 90° phase difference at desired frequency [13] as shown in Fig 3.1. The second method has been used in this project.
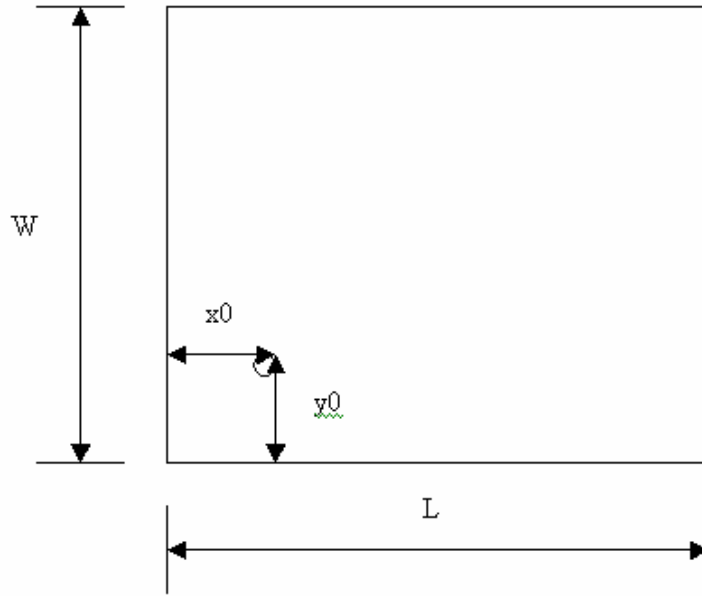
16

Figure 3.1: Circular Polarization with Singly Fed Patch

The cavity model can be used to approximate the ratio of orthogonal components of E field in far field region [2][13]

$$\frac{E_x}{E_y} = \frac{W(k^2 - k_{mn}^2)\cos(\pi x_0 / L)}{L(k^2 - k_{mn}^2)\cos(\pi y_0 / W)} \sin c(\frac{\pi D_x}{2L}) \qquad (3.22)$$

The ratio needs to be +j or –j for circular polarization

$$\frac{E_x}{E_y} = j \text{ for RHCP} \qquad (3.23)$$

$$\frac{E_x}{E_y} = -j \text{ for LHCP} \qquad (3.24)$$

17

4. Radiation Pattern

The radiated fields from a patch antenna for a given model, can be computed by assuming the four side-walls as the four narrow apertures or slots [5] as shown in Fig 4.1. The fields radiated by slots separated by length add along the principal E plane, which is the XY plane and principal H plane, which is the YZ plane in Fig 4.1, while the fields radiated by slots separated by width cancel each other. The slots are represented by equivalent electric current density $\mathbf{J_s}$ and magnetic current density, $\mathbf{M_s}$.
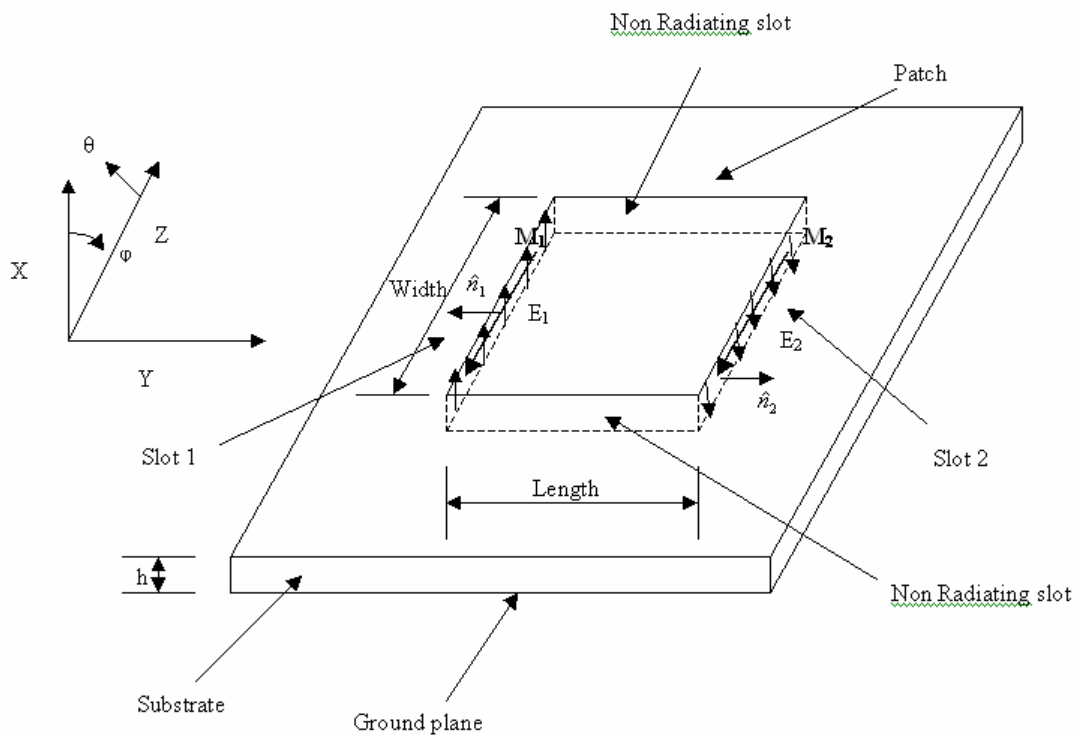

Fig 4.1 Microstrip Patch Antenna Radiating slots

If the electric and magnetic fields at the slot are $\mathbf{E_a}$ and $\mathbf{H_a}$, current densities are given by

$$\vec{J}_s = \hat{n} \times \vec{H}_a \qquad (4.1)$$

$$\vec{M}_s = -\hat{n} \times \vec{E}_a \qquad (4.2)$$

The cavity model assumes the perfect magnetic wall along the periphery of the region between the patch and ground plane, so the tangential components of magnetic field along the slots are assumed to be zero, and hence electric current density, $\mathbf{J_s}$ is taken as zero. So the radiated fields are computed based upon the magnetic current density, $\mathbf{M_s}$. The ground plane can be accounted for by using the image theory, which will double the magnetic current density given by equation 4.2 i.e

$$\vec{M}_s = -2\hat{n} \times \vec{E}_a \qquad (4.3)$$

Using the equivalence principle [5], each of the two radiating slots, radiates the same fields as a magnetic dipole with magnetic current density given by 4.3. The radiated fields are computed for one slot and then total fields are computed by multiplying with an array factor corresponding to two slots.

4.1 Radiated Fields for TM$_{01}$ mode

The radiated field from a slot of patch antenna is computed using the equivalent magnetic current density given by equation 4.3. By treating the slot as an aperture, the radiated fields are computed as [5]

$$E_r \approx E_\theta \approx 0 \qquad\qquad\qquad (4.4)$$

$$E_\phi = +j \frac{k_0 h W E_0 e^{-jk_0 r}}{2\pi r} \left[\sin\theta \frac{\sin(X)}{X} \frac{\sin(Z)}{Z} \right] \qquad (4.5)$$

$$\text{where } X = \frac{k_0 h}{2} \sin\theta \cos\phi \qquad\qquad\qquad (4.6)$$

$$Z = \frac{k_0 W}{2} \cos\theta \qquad\qquad\qquad (4.7)$$

The array factor for two elements of same magnitude and phase, separated by a distance L_{eff} along y axis is given by

$$AF = 2\cos\left(\frac{k_0 L_{eff}}{2} \sin\theta \sin\phi \right) \qquad (4.8)$$

Multiplying 4.5 and 4.8, and assuming $k_0 h \ll 1$, and putting $V_0 = hE_0$, where V_0 is voltage across the slot, gives

$$E_\phi = +j \frac{2 V_0 e^{-jk_0 r}}{\pi r} \left[\sin\theta \frac{\sin(\frac{k_0 W}{2}\cos\theta)}{\cos\theta} \right] \cos\left(\frac{k_0 L_{eff}}{2} \sin\theta \sin\phi \right) \qquad (4.9)$$

The equation 4.9 is used in this project to compute and plot the radiation pattern for patch antenna.

4.2 Antenna Array

The radiation pattern from a single patch antenna or any typical antenna element for that matter is typically very wide. The arrays of antennas are typically used to obtain the desired directivity. The arrays are used for beam scanning applications also, where the maxima of beam is pointed in different directions by adjusting the relative phase differences between elements of array.

The most common arrangement of elements is a linear array, with uniform amplitude and constant progressive phase difference between elements. A number of such linear arrays can be placed besides each other to form a planar array. In this project, we use the planar array, with uniform amplitude and constant progressive phase difference between elements as shown in Figure 4.2.
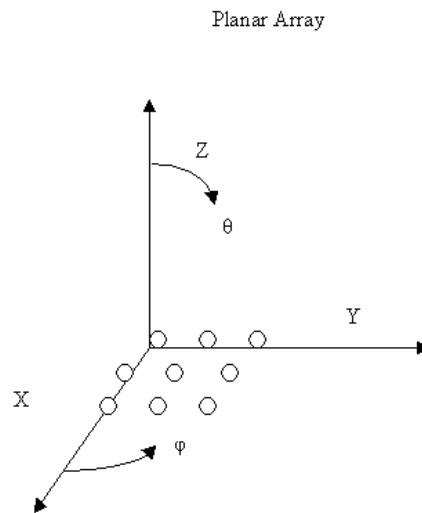
Planar Array

Figure 4.2 Planar Array

4.2.1 Array Factor for Planar Array

Consider a linear array of M elements placed along x axis, separated from previous element by distance, d_x, with uniform amplitude I_0 and constant progressive phase different β_x. The array factor for such an arrangements is given by

$$AF = I_0 \sum_{m=1}^{M} e^{j(m-1)(kd_x \sin\theta \cos\phi + \beta_x)} \qquad (4.10)$$

Now consider N such arrays placed along y axis, separated by distance d_y with progressive phase difference of β_y. The array factor for such an array is given by

$$AF = I_0 \sum_{m=1}^{M} e^{j(m-1)(kd_x \sin\theta \cos\phi + \beta_x)} \sum_{n=1}^{N} e^{j(n-1)(kd_y \sin\theta \sin\phi + \beta_y)} \qquad (4.11)$$

The normalized form of 4.11 can be expressed as

$$AF_n(\theta,\phi) = \left[\frac{1}{M} \frac{\sin(\frac{M}{2}\psi_x)}{\sin(\frac{\psi_x}{2})} \right] \left[\frac{1}{N} \frac{\sin(\frac{N}{2}\psi_y)}{\sin(\frac{\psi_y}{2})} \right] \qquad (4.12)$$

where $\quad \psi_x = kd_x \sin\theta \cos\phi + \beta_x \qquad (4.13)$

$\psi_y = kd_y \sin\theta \sin\phi + \beta_y \qquad (4.14)$

The normalized form of array factor is used for polar plots described in next chapter.

5. Matlab Implementation

The equations developed in chapter 3 for input impedance and circular

polarizations, and in chapter 4 for radiation pattern of patch antenna and array factor,

have been used to implement a Matlab Graphical user Interface based patch antenna

design software. Three pieces of software have been developed, the code is available in

appendix C.

a)   The first software has rectangular plots for return loss, axial ratio and

phase difference between two orthogonal E field components.

b)   The second software has 2D polar plots for patch antenna radiation

pattern. It also has polar plot for array factor and a polar plot for total

pattern, obtained by multiplication of element pattern and array pattern.

c)   The third software has 3D polar plots for items mentioned in b).

5.1 Cavity Model Based Simulation Software

The cavity model based simulator use equations 3.6, 3.9 – 3.11, and 3.14 – 3.21 to

compute the input impedance for a coaxial fed rectangular patch antenna. The return loss,

|S11| is computed as

$$|S11| = \left| \frac{Z_{in} - 50}{Z_{in} + 50} \right| \qquad (5.1)$$

|S11| in db is plotted on rectangular axis versus user entered frequency sweep.

Equation 3.22 is used to compute the axial ratio and phase difference between two

orthogonal components of E field. The axial ratio is plotted in db and phase difference is

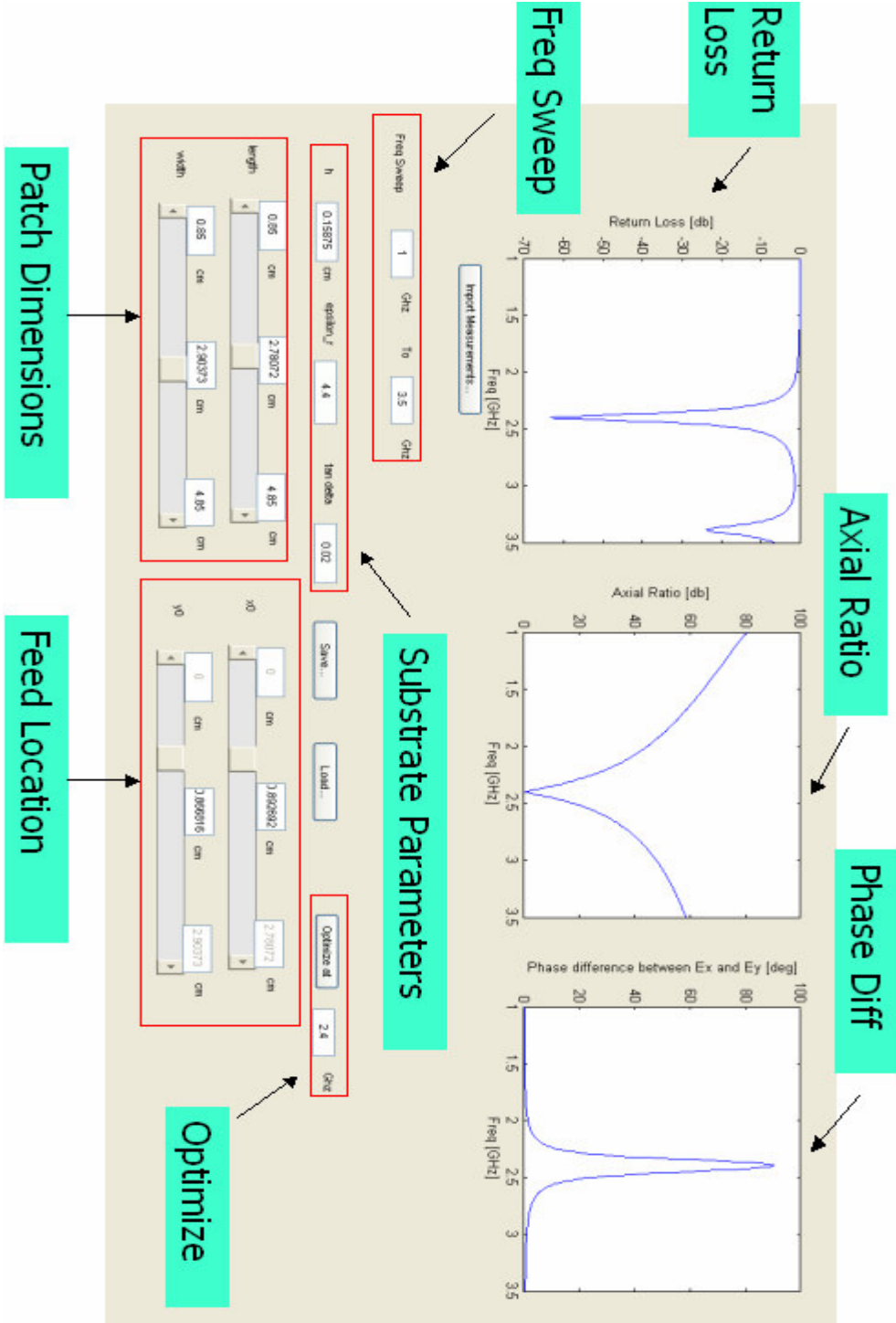plotted in degress v/s frequency sweep.

Figure 5.1 Cavity based Simulator Graphical User Interface

Figure 5.1 shows the GUI for cavity-based simulator. The upper portion of interface has three rectangular plots mentioned above. The frequency range used in the three plots and the parameters for patch antenna as entered in lower portion of interfaces

a) The edit fields labeled as "Freq Sweep" in Figure 5.1 allows entering of frequency range in GHz.

b) There are three edit fields labeled as "Substrate Parameters" in Figure 5.1. The field called h allows entering the height of substrate in cm. The field called epsilon_r allows entering the relative permittivity of the substrate. The field called tan delta allow entering the loss tangent.

c) The GUI has sliders for length and width of the patch and for x and y coordinate of location of coaxial feed, labeled as "Patch Dimensions and Feed Location" in Figure 5.1. The sliders allow the user to easily change these parameters in the specified range to immediately see the affect of these parameters on return loss, axial ratio and phase difference. User can set the min and max limits for sliders corresponding to length and width. The min for feed location sliders is automatically set to 0 and max is set to length and width.

d) The GUI of Figure 5.1 can be used to design either linear polarized or circularly polarized patch antenna. For linear polarization, the return loss is the only relevant characteristics in this interface. The patch dimensions and feed location can easily be tuned to achieve the desired return loss. On the other hand, to design for circular polarization, along with return loss, axial ratio needs to tuned to 0 db and phase difference between two orthogonal components of E fields needs to be

tuned to either $+90^0$ or -90^0. It is very difficult to manually tune four parameters to obtain the appropriate values for three outputs. To help with that, Optimize button has been provided. Clicking on the Optimize button optimizes all three characteristics by varying the patch dimensions and feed locations within the limits set by user. The current values of patch dimensions and feed location are fed as initial values to the optimizer. The implementation use Matlab's multi-objective goal attainment function, called fgoalattain.

e) Once the patch antenna has been tuned to obtain the desired characteristics, it can be saved by clicking on the Save button. The saved design can then be opened later by clicking on the Open button and selecting the earlier saved design.

f) The Import Measurements button allow importing of measurements values to compare with simulation values.

5.2 2D Radiation Pattern and Array Pattern

The second piece of software uses equation 4.9 to plot the radiation pattern of the patch antenna on a polar plot. The θ and φ are as defined in the coordinate system in Figure 4.1. The software uses equations 4.12 – 4.14 for plotting the array pattern on polar axis. The array pattern and patch element pattern are the multiplied together to obtain the total pattern. The software allows designing planar or linear arrays of patch antenna and obtain the polar radiation pattern plots.
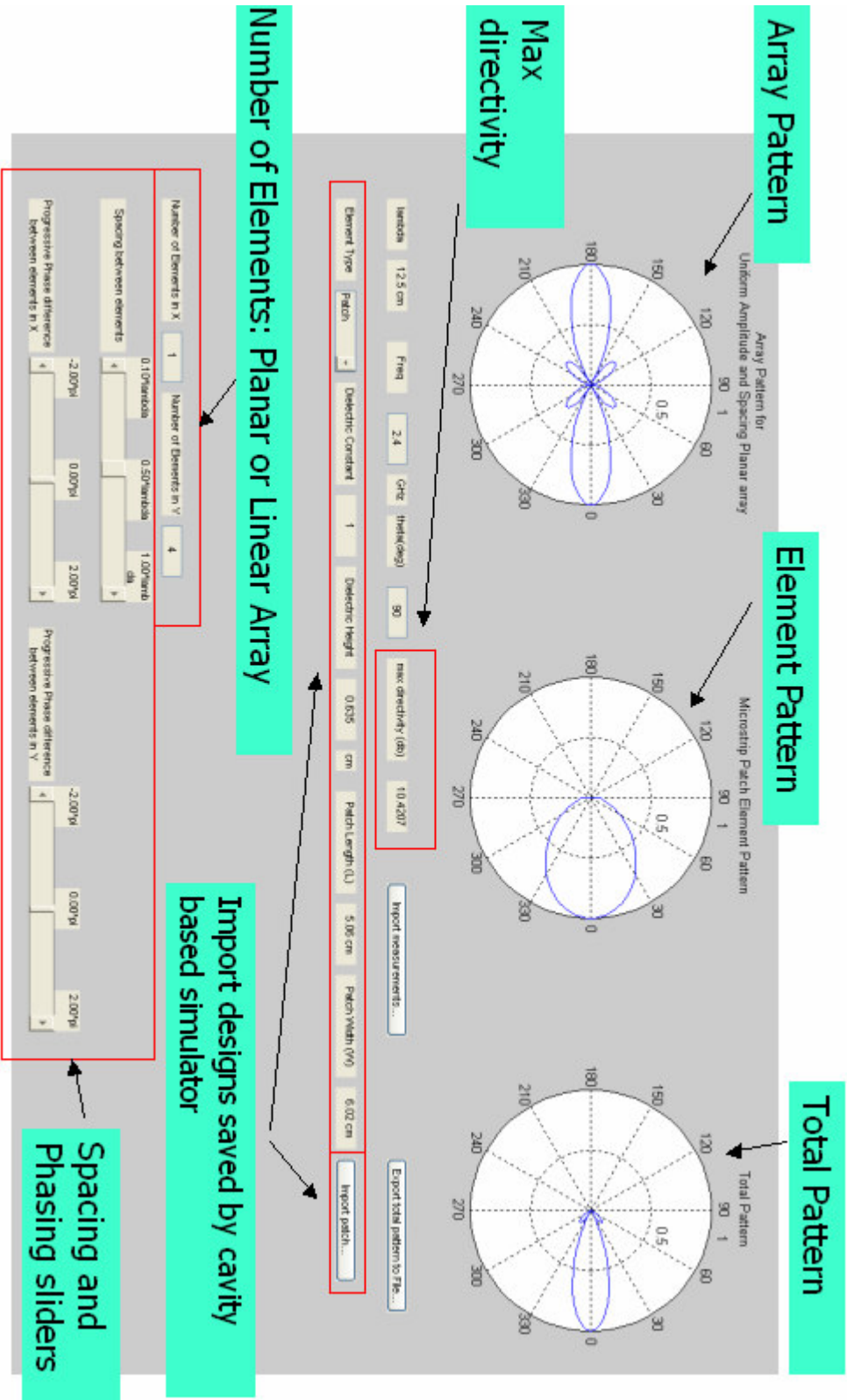
Figure 5.2 2D Radiation Pattern

Figure 5.2 shows the GUI for 2D radiation pattern software. The upper portion has polar plots for element pattern, array pattern and total pattern v/s φ. θ can be entered in the edit field called theta.

a) The edit field called Freq allows entering the frequency for the patch antenna. The frequency should be entered as the first step of using this interface. The non editable text field called lambda, updates to correct wavelength in cm, as frequency is entered in GHz.

b) The patch design file saved by cavity simulator can directly be opened in this interface by clicking on Import Patch button and selecting the design file. The parameters of patch are populated in fields called Dielectric Constant, Dielectric Height, Patch Length and Patch Width.

c) The lower portion of the interface allows designing a linear or planar array as in Fig 4.2. The number of elements in X and Y direction can be enetered. X and Y are as defined in the coordinate system in Figure 4.2.

d) The sliders for phasing and spacing allow setting the distance between elements of array and progressive phase difference between them.

e) Import Measurements button allows importing the measurement data to compare with simulation data.

f) The total pattern can be exported to a file by clicking on Export Total Pattern to File. The exported pattern can then be used as the element pattern by selecting the Element Type as Imported. This ability can be used to complex array configurations.

Figure 5.3 shows the GUI for 3D radiation pattern software. All the
parameters in this software are same as in 2D version except that it has 3D
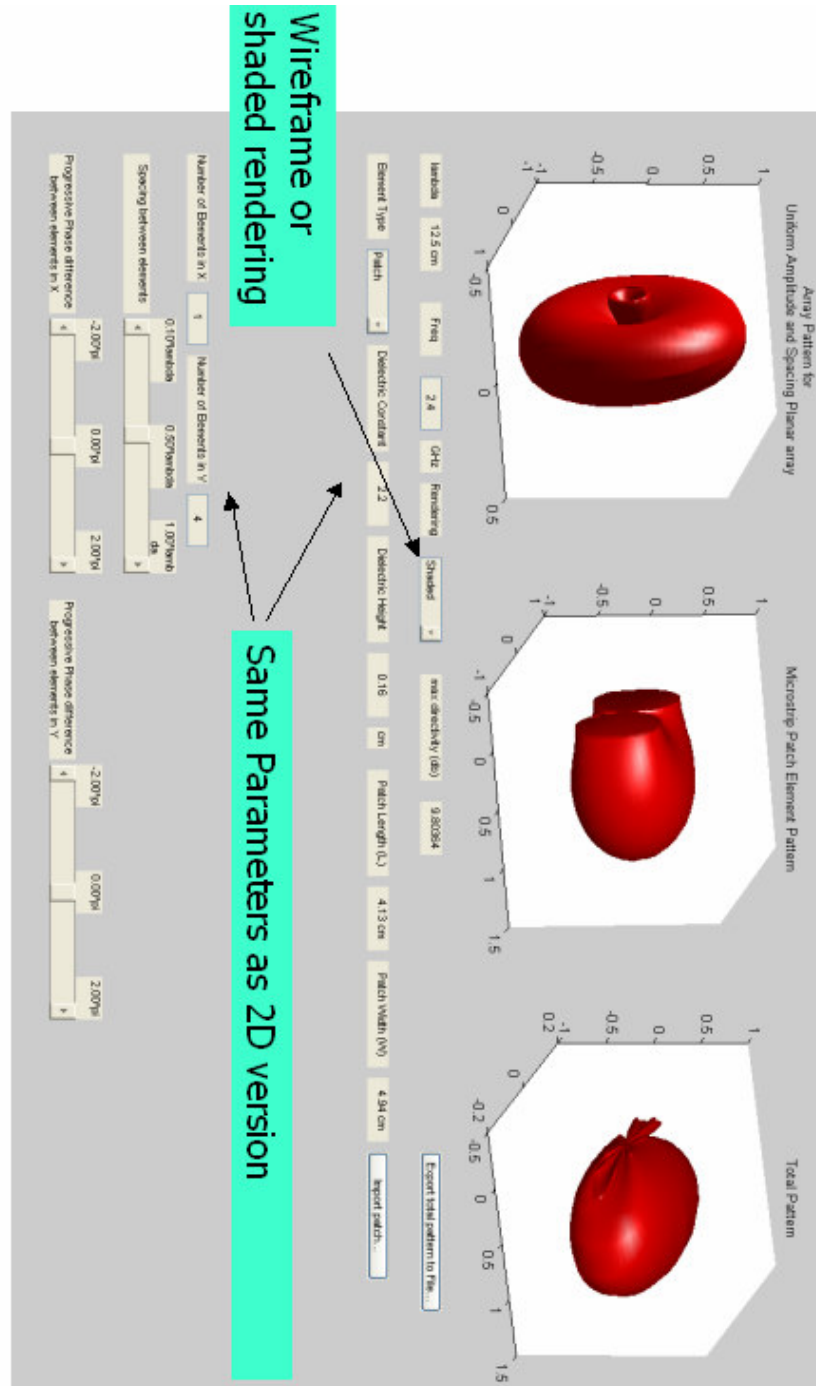polar plots. It allows user to plot either wireframe or shaded plots.

Figure 5.3 3D Radiation Pattern

6. Fabrication and Measurements

Two test antennas have been made to validate the simulation results obtained from the developed software. Both of them use substrate as air. The first antenna is 2.4 GHz single band circularly polarized antenna. The second antenna is 2.4, 5.8 GHz two-layered dual band circularly polarized antenna. The lower layer is designed for 2.4 GHz and upper layer for 5.8 GHz. The lower layer also acts as ground plane for upper layer. The antennas are shown in Figure 6.1 and 6.2.
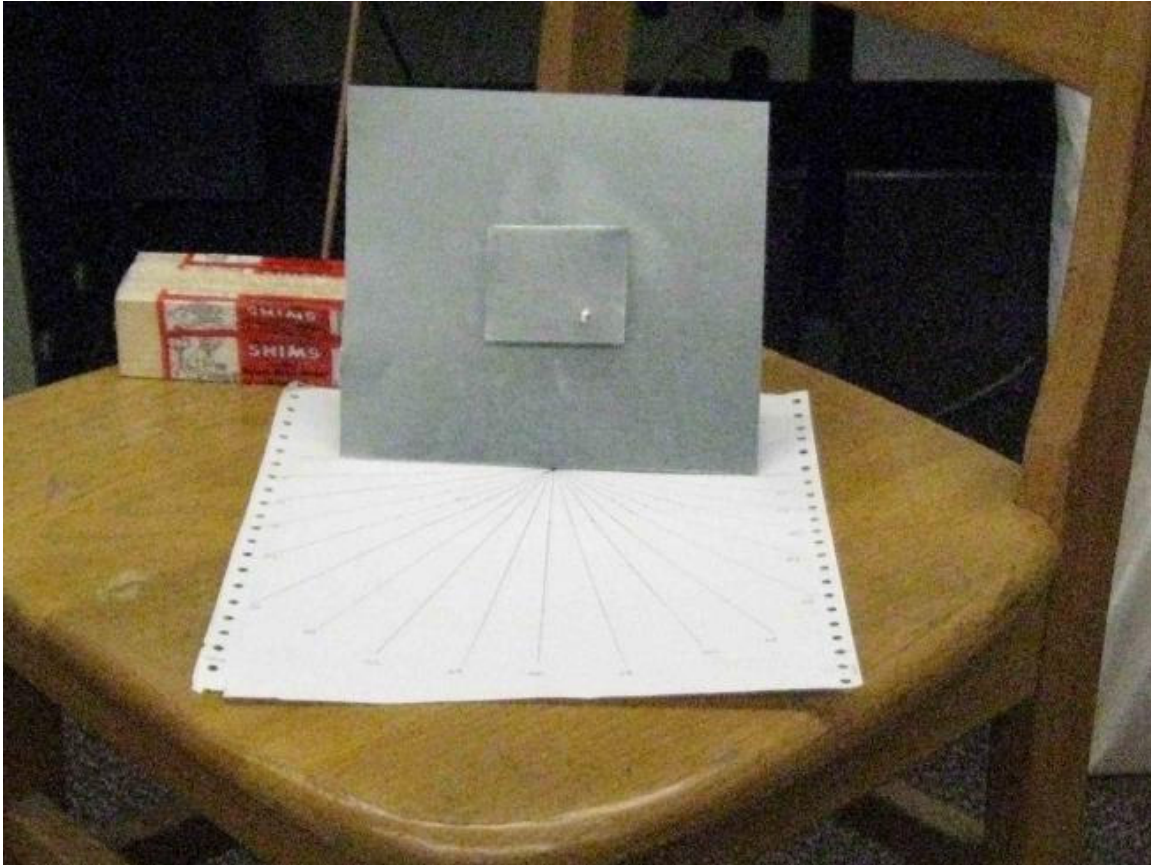
Figure 6.1: 2.4 GHz circularly polarized test antenna
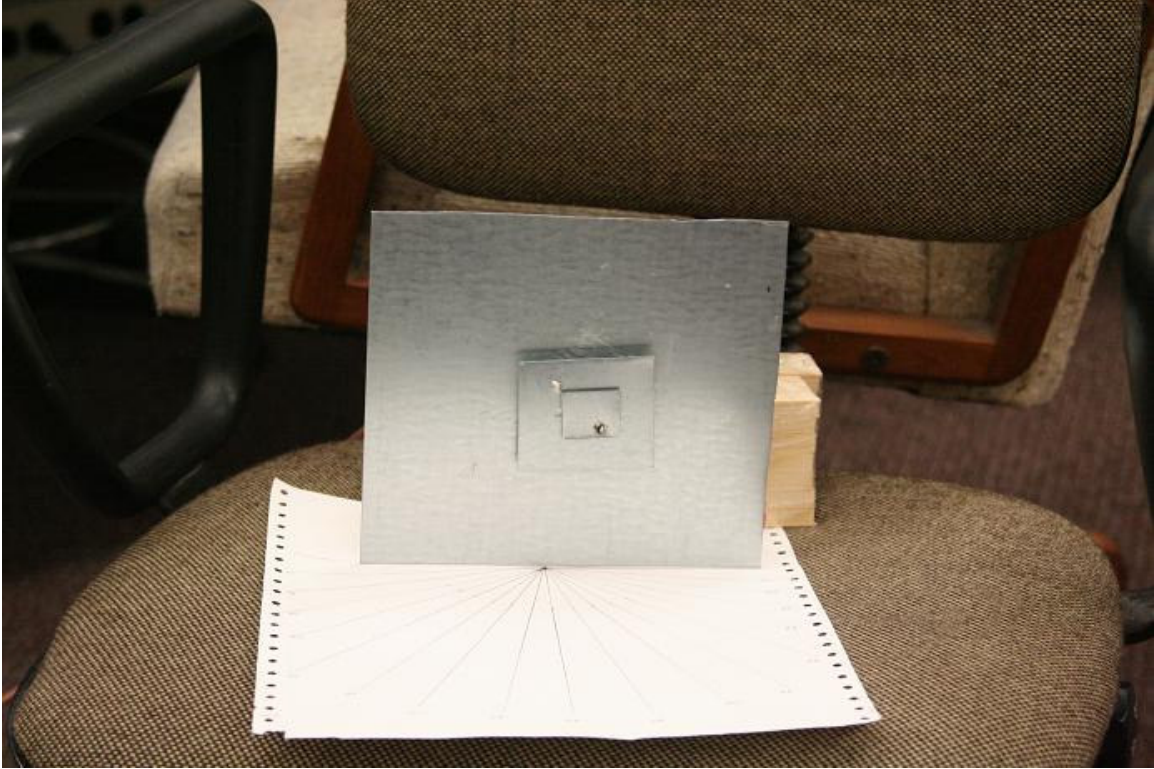
Figure 6.2: 2.4, 5.8 GHz dual band circularly polarized test antenna

The test antennas are simulated in the cavity simulator. Return loss, axial ratio and phase difference are optimized using the "Optimize" button. The results of simulation and the design parameters for 2.4 GHz and 5.8 GHz are shown in Figure 6.3 and 6.4.
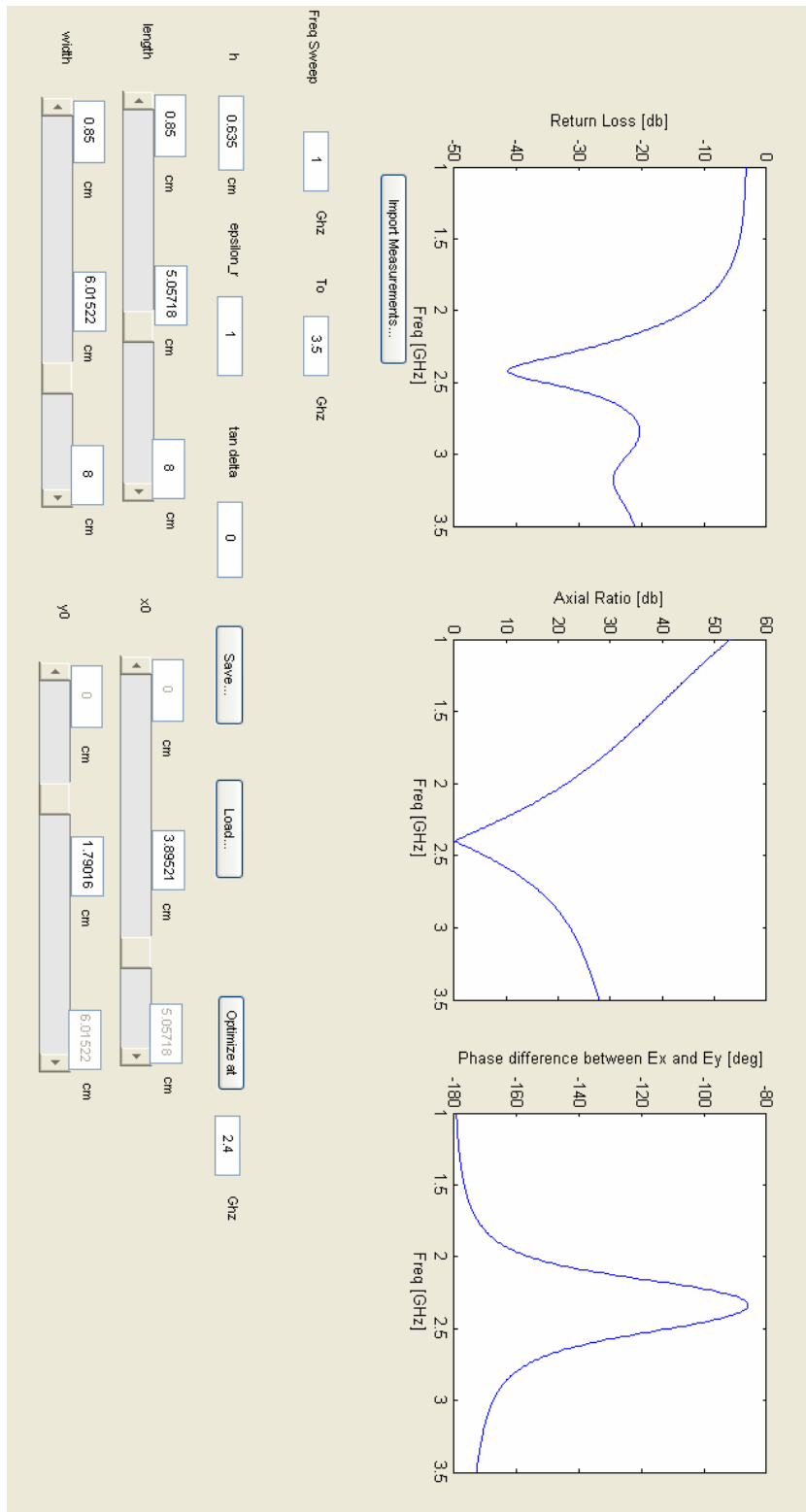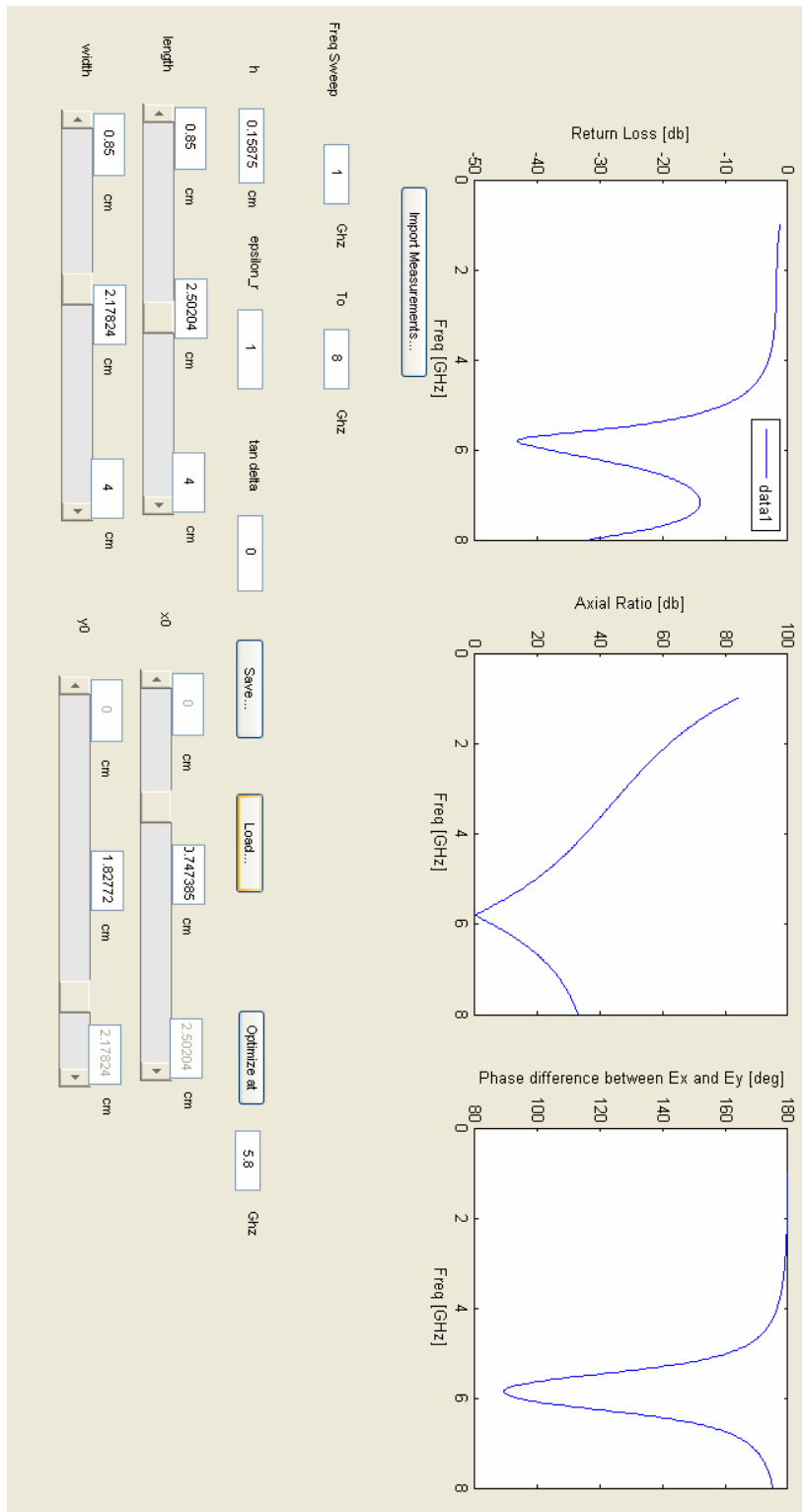
Figure 6.3 Simulation of 2.4 GHz band

Figure 6.4 Simulation of 5.8 GHz band

6.1 Measurements

The measurements on test antennas have been done using the Network Analyzer in E347 lab. The return loss is obtained by connecting the test antenna to one of the ports of network analyzer. The radiation pattern has been estimated by measuring the insertion loss using test antenna as radiator and a dipole as receiver. The radiation pattern measurements has been taken at three locations and averaged out to reduce the multi path affects.

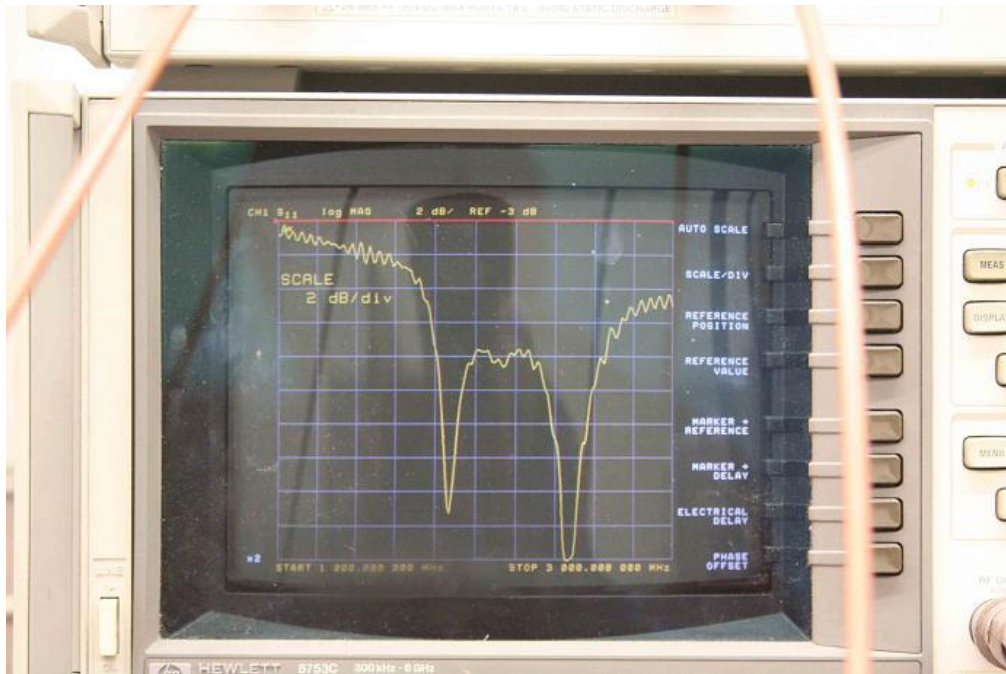**Figure 6.5: Measurements with Network analyzer in E347 lab**

Figure 6.6: Return Loss Measurement with network analyzer in E347 lab

The circular polarization has been measured by taking the radiation pattern readings in two orthogonal positions of antennas as shown in Figure 6.6. All the measurement data is available in Appendices A1 to B3.
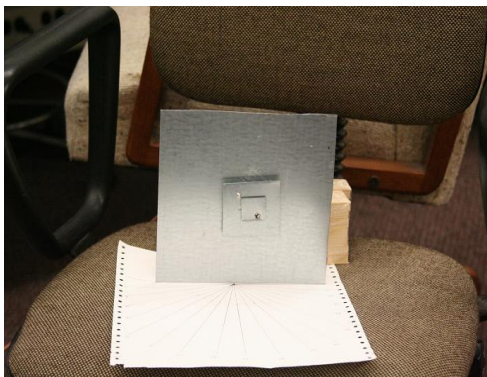

Figure 6.7: Measurement for circular polarization

6.2 Comparison of Simulation with Measurement Results for Single Band Antenna

The measured return loss data has been compared with simulation results by using the Import Measurements functionality and overlaying the measurement data over simulation results. The comparison for 2.4 GHz single band antenna is shown in Figure 6.7.
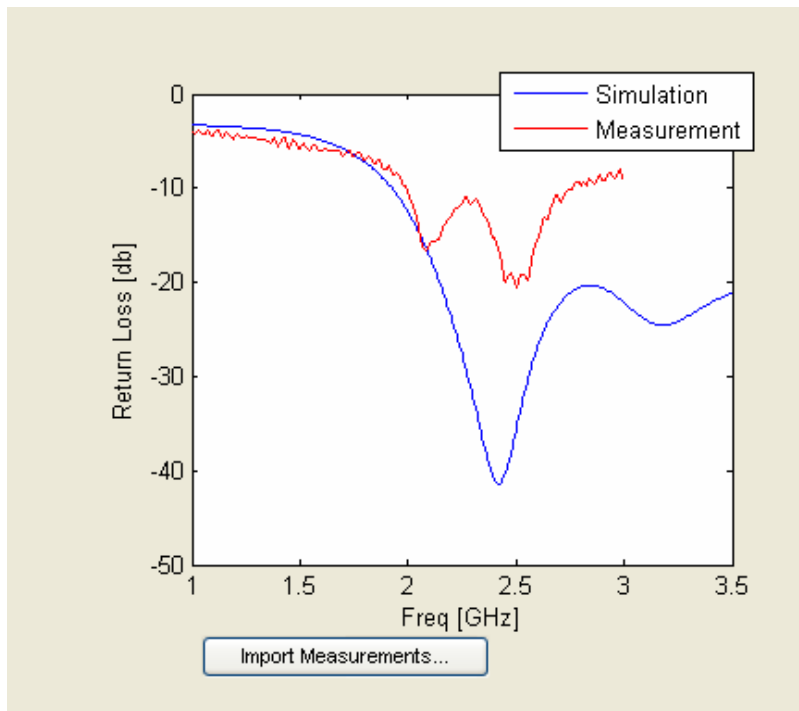

Figure 6.8: Return Loss Comparison for 2.4 GHz single band antenna

6.2.1 Analysis of Return Loss Measurement Results

The measured return loss shows two peaks close to 2.4 GHz. The two peaks are possibly the result of improper matching of two modes, being excited for circular

polarization, in the fabricated antenna. The test antenna has been fabricated with hand, and there is a tolerance of 2 to 3mm at the solder joint location of feed point with the patch element. The difference in the magnitude of return loss between measured and simulated results is also due to the fabrication tolerance. In order to account for fabrication tolerance, the feed location was perturbed in the simulations by 2 to 3mm and worst-case scenario is plotted as shown in Figure 6.8. The measured results show better correlation with the simulations.
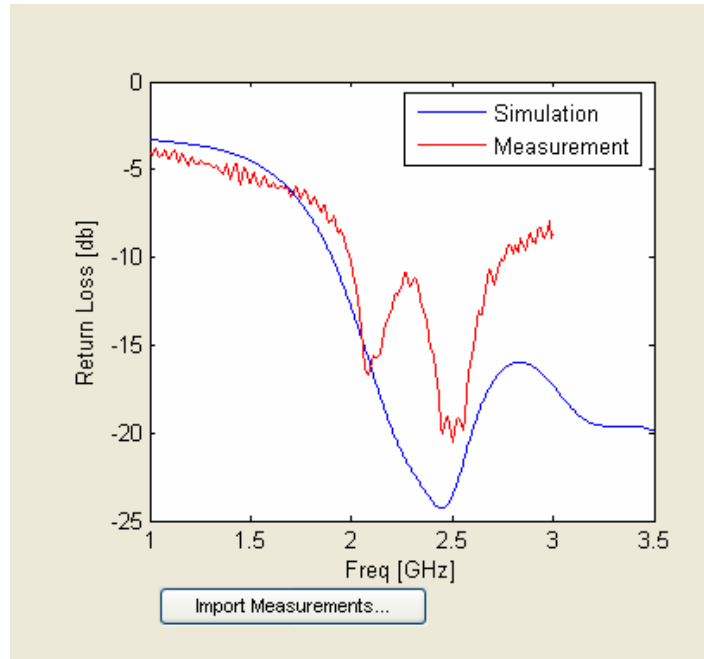

Figure 6.9: Return Loss Comparison for 2.4 GHz single band antenna with probe location 3mm off from optimized value

6.2.2 Comparison of radiation pattern results

The radiation pattern measurements taken in db, at multiple locations are averaged out and converted to normalized fraction values to overlay on simulation results on polar plots. Figure 6.9 shows the comparison of measured values with simulation values. The comparison shows close agreement.
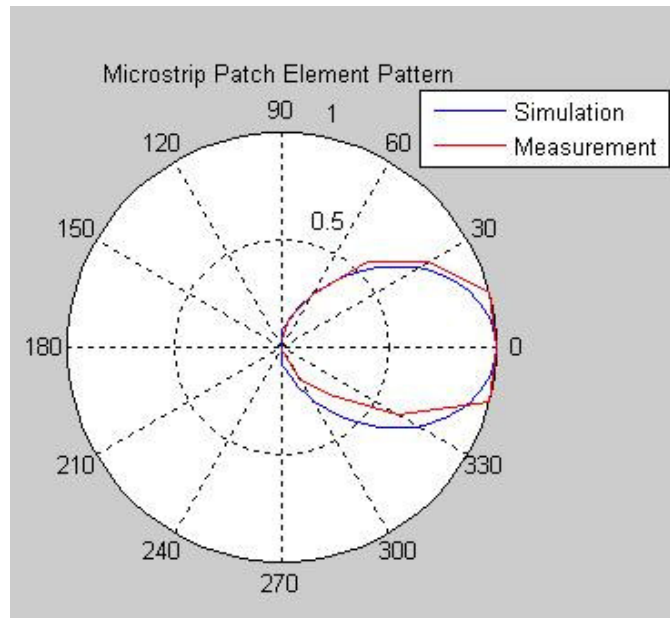

Figure 6.10: Radiation Pattern Comparison for 2.4 GHz single band antenna

The measured axial ratio is plotted in db by taking the difference between the radiation values for the two orthogonal positions of antenna as illustrated in Figure 6.6. The measured axial ratio for 2.4 GHz single band antenna is shown in Figure 6.10. The axial ratio is close to 6db instead of 0db. This is also attributed to improper matching of two modes, being excited for circular polarization due to fabrication tolerance.
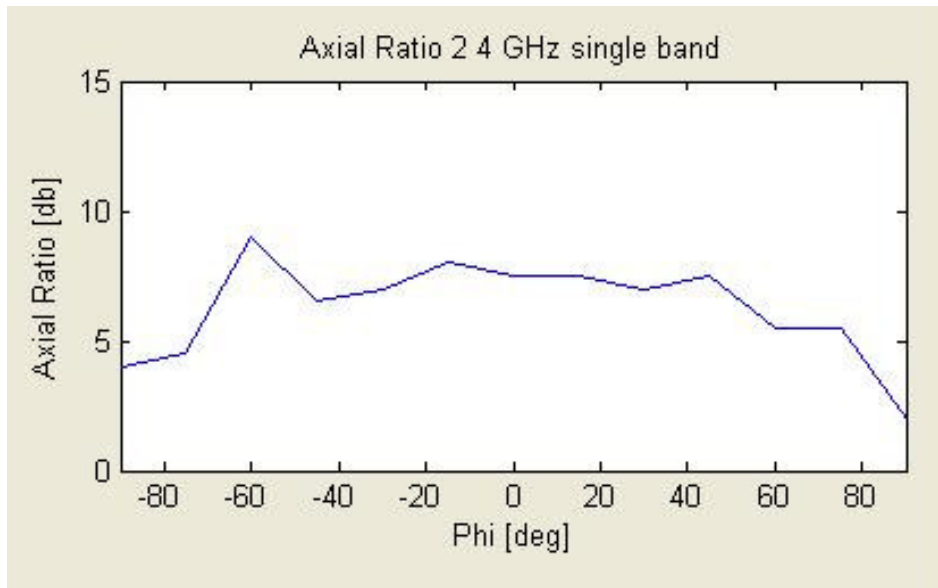
Figure 6.11: Measured Axial Ratio for 2.4 GHz single band antenna

6.3 Comparison of Simulation with Measurement Results for Dual Band Antenna

The measurements for dual band antenna have been done for both bands in a manner similar to single band antenna. The return loss, radiation pattern and axial ratio for both bands are shown in Figure 6.11 to Figure 6.16. The comparisons for results are similar as for 2.4 GHz antenna, with one exception. The resonance for 5.8 GHz antenna is closer to 5.5 GHz. One reason for shift in resonance is the fabrication tolerance mentioned in previous section. Another possible reason is that the ground plane for 5.8 GHz patch is 2.4 GHz patch, which is relatively small and is not large enough to assume infinite. The simulations however do not take into account the finite ground plane affects.
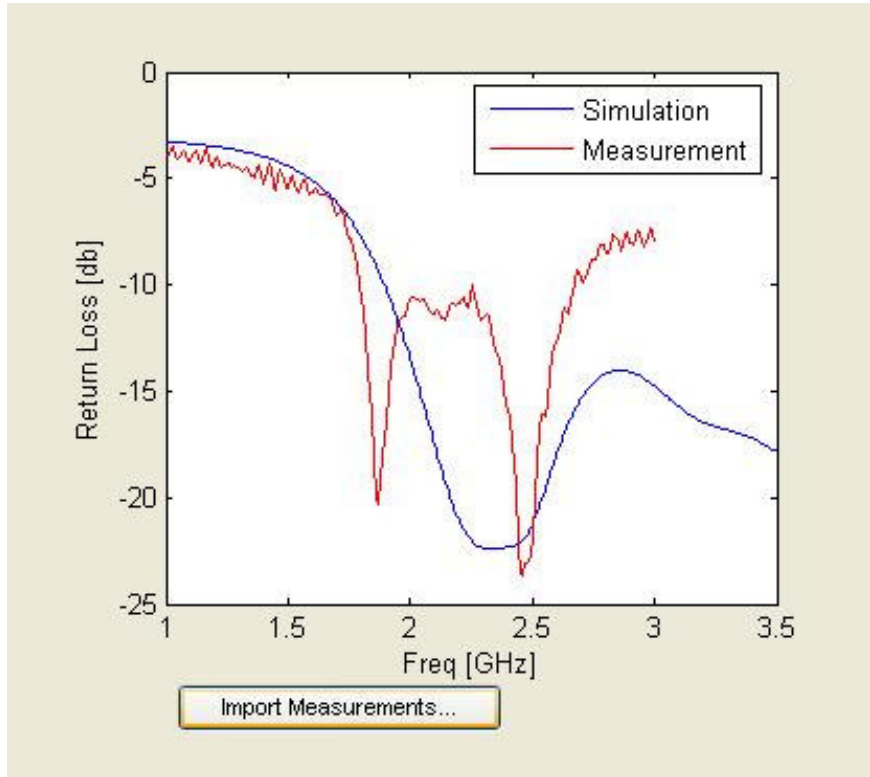
Figure 6.12: Return Loss Comparison for 2.4 GHz band of dual band

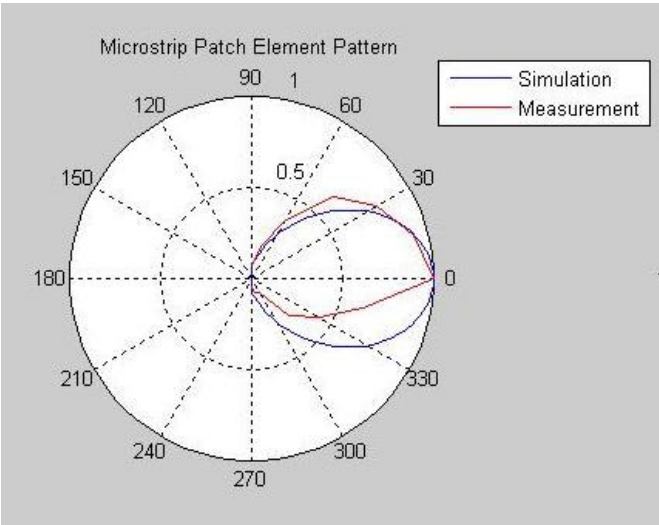**antenna with probe location 3mm off from optimized value**

Figure 6.13: Radiation Pattern Comparison for 2.4 GHz band of dual band
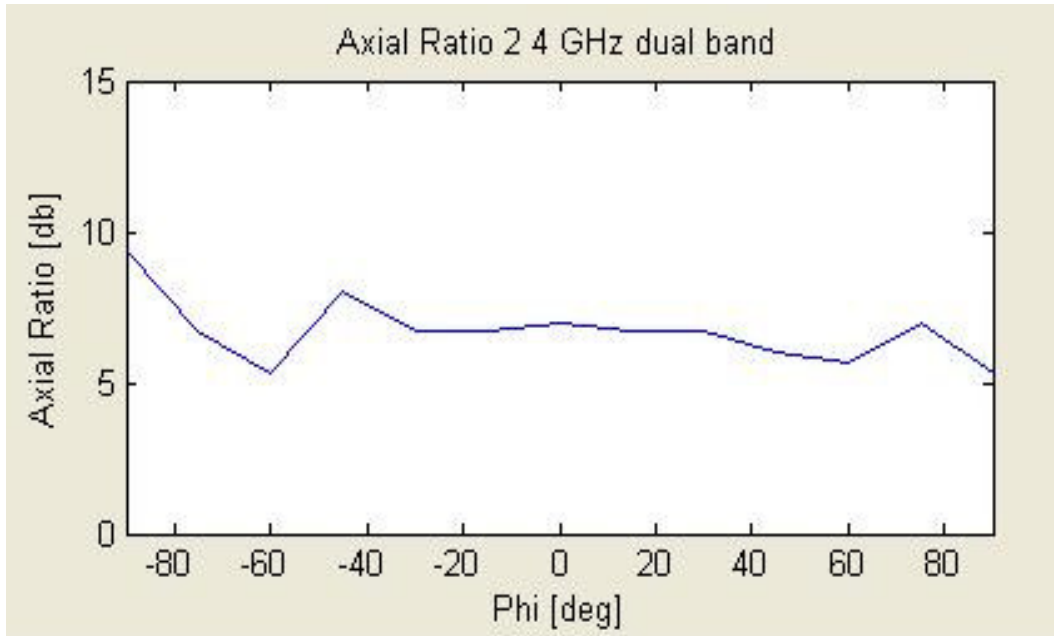
antenna

Figure 6.14: Measured Axial Ratio for 2.4 GHz single band antenna
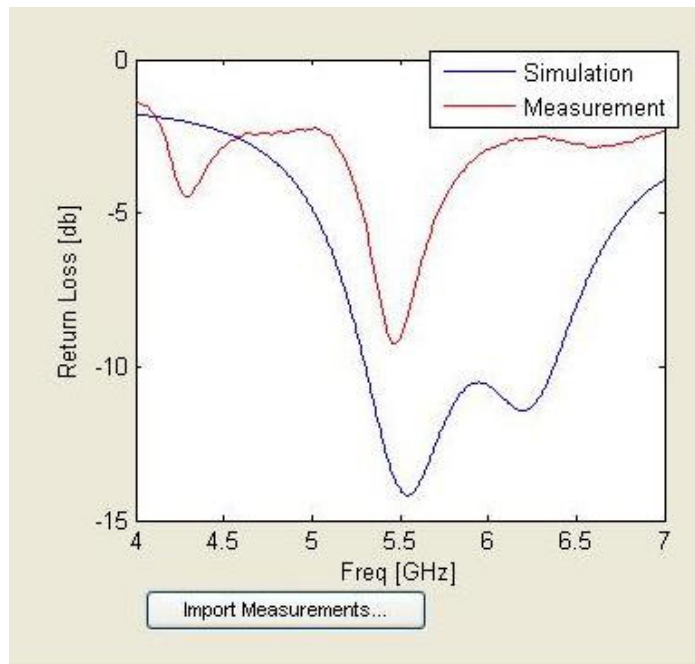

Figure 6.15: Return Loss Comparison for 5.8 GHz band of dual band antenna with probe location 3mm off from optimized value
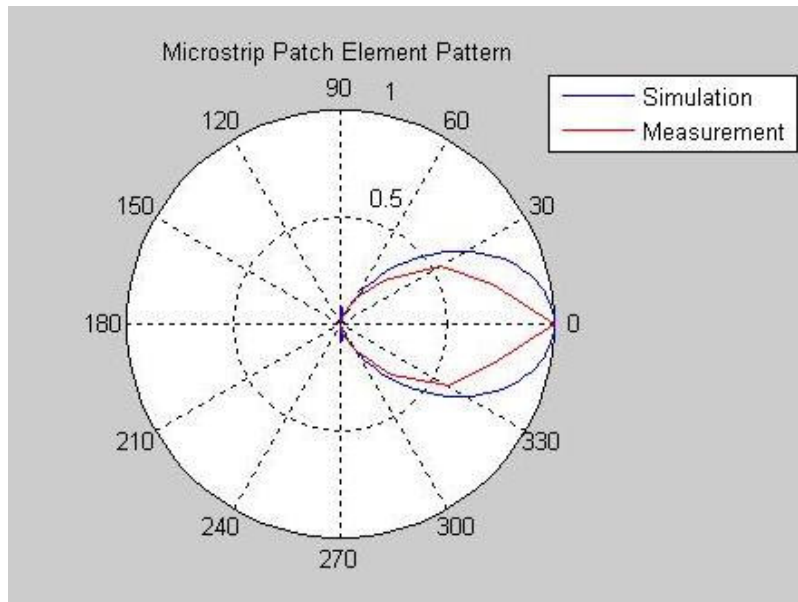
Figure 6.16: Radiation Pattern Comparison for 5.8 GHz band of dual band antenna
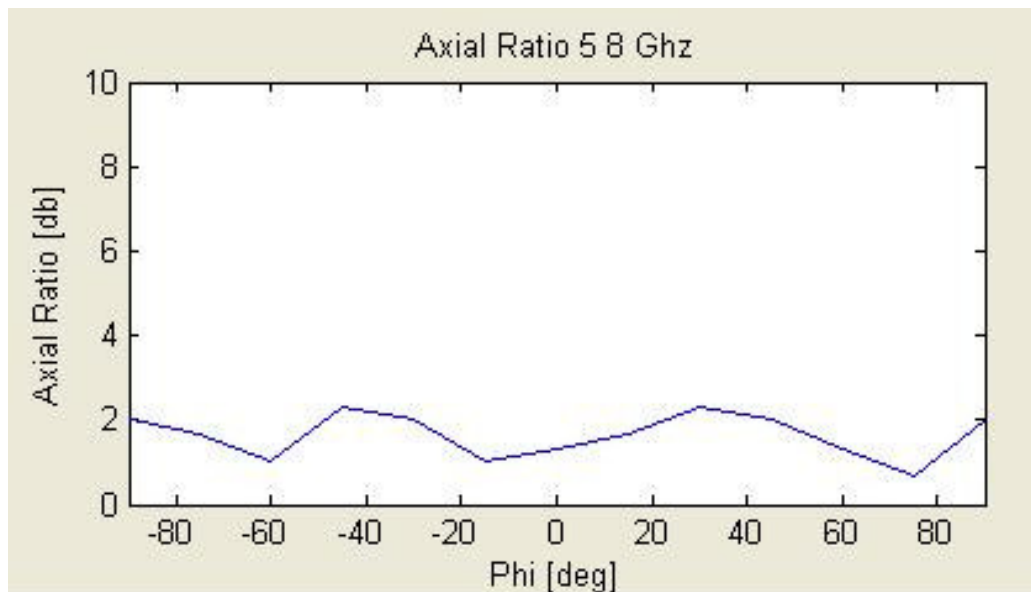

Figure 6.17: Measured Axial Ratio for 5.8 GHz single band antenna

7. Conclusions

In this project, a Matlab GUI based simulation software to simulate microstrip patch antennas has been developed.

a)   The simulation software has ability to predict return loss, radiation pattern and circular polarization

b)   The simulation software can be used to design dual band antennas.

c)   The simulation software allows simulation of antenna arrays

A single band antenna and a dual band antenna have been fabricated, and return loss and radiation pattern measurements have been done. The measurement results agree with simulation results within the limitations of fabrication method used.

8. Future Work

The work done in this project can be extended in multiple ways.

a) The simulations for dual band antennas can be improved by accounting for the finite ground plane affects.

b) The radiation patterns plotted are for one particular mode. The software should allow user to select the mode and it should then plot the radiation pattern for that mode

c) The software can allow plotting the input impedance on Smith Chart.

REFERENCES

[1] Lo, Y. T., Solomon, D., and Richards W.F., 'Theory and Experiment on Microstrip antennas.' IEEE Trans. on AP, 1979, Vol. AP-27, pp. 137 – 149.

[2] Richards W.F., Lo, Y. T., and Harrison D. D., 'An Improved theory for Microstrip antennas and Application.' IEEE Trans. on AP, 1981, Vol. AP-29, pp. 38 – 46.

[3] Garg, R., Bhartia, P., Bahl, I., and Ittipiboon, A., Microstrip Antenna Design Handbook, Artech House, Inc, 2001.

[4] Stutzman, W.L., and Thiele, G.A., Antenna Theory and Design, John Wiley & Sons, Inc, 1998.

[5] Balanis, C.A., Antenna Theory, Analysis and Design, John Wiley & Sons, Inc, 1997.

[6] Pozar, D. M., Microwave Engineering, Second Edition, JohnWiley & Sons, Inc, 1988.

[7] Gan, Yeow-Beng, Chua Chee-Parng, and Li, Le-Wei , An enhanced cavity model for microstrip antennas, Microwave and optical technology letters, vol. 40, no. 6, March 20 2004, pp. 520 – 523.

[8] Thouroude, D., Himdi , M. and Daniel, J. P., CAD-Oriented Cavity Model For Rectangular Patches, Electronics Letters 2lst June 1990 Vol. 26 No. 13, pp. 842 - 844

[9] D. D. Sandu, O. G. Avadanei, A. Ioachima, D. Ionesi, Contribution To The Cavity Model For Analysis of Microstrip patch antennas, Journal of Optoelectronics and advanced materials vol. 8, no. 1, Febraury 2006, p. 339 – 344

[10] Martin, N. M., Improved cavity model parameters for calculation of resonant frequency of rectangular microstrip antennas, Electronic Letters, 26th May 1988, Vol. 24, No. 11, pp. 680-681

[11] Deshpande, M. D., Bailey, M. C., Input impedance of microstrip antennas, IEEE transactions on antennas and propagation, vol. Ap-30, no. 4, July 1982, pp. 645 – 650

[12] James, J.R. and Hall, P.S., Handbook of Microstrip Antennas, Vols 1 and 2, Peter Peregrinus, London, UK, 1989.

[13] Bancroft, Randy, Microstrip and Printed Antenna Design, 2nd Edition, SciTech Publishing Inc., 2009

[14] Pozar, D. M. and Schaubert, D. H., Microstrip Antennas, The Analysis and Design of Microstrip Antennas and Arrays, IEEE Press, 1995

[15] Derneryd, A. G. and Lind, A. G., Extended Analysis of Rectangular Microstrip Resonator Antennas, IEEE transactions on antennas and propagation, Vol. AP-27, No. 6, November 1979, pp. 846 – 849

[16] Hammerstad, E. O., Equations for microstrip circuit design, Proc. Fifth European Microwave Conf., pp. 268-272, September 1975.